ARTICLES

nature structural & molecular biology

Structural basis for distinct ligand-binding and targeting properties of the receptors DC-SIGN and DC-SIGNR

Yuan Guo[1,5], Hadar Feinberg[2,5], Edward Conroy[1], Daniel A Mitchell[1], Richard Alvarez[3], Ola Blixt[4], Maureen E Taylor[1], William I Weis[2] & Kurt Drickamer[1]

Both the dendritic cell receptor DC-SIGN and the closely related endothelial cell receptor DC-SIGNR bind human immunodeficiency virus and enhance infection. However, biochemical and structural comparison of these receptors now reveals that they have very different physiological functions. By screening an extensive glycan array, we demonstrated that DC-SIGN and DC-SIGNR have distinct ligand-binding properties. Our structural and mutagenesis data explain how both receptors bind high-mannose oligosaccharides on enveloped viruses and why only DC-SIGN binds blood group antigens, including those present on microorganisms. DC-SIGN mediates endocytosis, trafficking as a recycling receptor and releasing ligand at endosomal pH, whereas DC-SIGNR does not release ligand at low pH or mediate endocytosis. Thus, whereas DC-SIGN has dual ligand-binding properties and functions both in adhesion and in endocytosis of pathogens, DC-SIGNR binds a restricted set of ligands and has only the properties of an adhesion receptor.

Two distinct roles have been ascribed to the dendritic cell receptor DC-SIGN: it is believed to function in the initial recognition of pathogens by dendritic cells and also mediates adhesion of T cells that scan the surface of the dendritic cells for the presence of peptide antigens[1,2]. The latter interaction involves binding to intercellular adhesion molecule 3 (ICAM-3); this originally led to the receptor's designation as dendritic cell–specific ICAM-grabbing nonintegrin[3]. Although the epitopes required for binding to ICAM-3 have not been defined, the recognition of pathogens is believed to involve binding of surface carbohydrates.

The presence of C-type carbohydrate-recognition domains (CRDs) in DC-SIGN is consistent with the receptor's role in the recognition of carbohydrate ligands. Binding to high-mannose oligosaccharides underlies the interaction of DC-SIGN with enveloped viruses[4] including human immunodeficiency virus (HIV), hepatitis C virus and Ebola virus[5,6]. Binding of HIV to DC-SIGN on dendritic cells enhances the infection of T cells[3,7]. This type of *trans* presentation may also occur for other viruses, but in some cases DC-SIGN can serve directly as a route for infection of cells[8,9]. The interaction of DC-SIGN with mannose-containing glycans underlies the dendritic cell binding of *Mycobacterium tuberculosis*, the yeast *Candida albicans* and *Leishmania* parasites[5,6]. DC-SIGN also binds to fucose-containing glycans[10] including those found on schistosomes and *Helicobacter pylori*[11]. Bound *C. albicans* are internalized into the dendritic cells[12], but the fate of bound pathogens has not been extensively explored.

In humans, DC-SIGN is expressed in alveolar and decidual macrophages, lymph node sinus endothelial cells, and Hofbauer cells in the placenta in addition to dendritic cells. A closely related receptor, DC-SIGNR or L-SIGN, is found on endothelial cells in liver, lymph nodes and placenta[13]. Both receptors are tetrameric type 2 transmembrane proteins in which the C-terminal CRDs are separated from the membrane by an extended region containing α-helices[4]. DC-SIGNR shares with DC-SIGN the ability to bind high-mannose oligosaccharides and can serve as a receptor for many of the same viruses[4,7–9]. Binding to DC-SIGNR can also increase the efficiency of HIV infection of T cells. Thus, there seems to be some overlap in the behavior of the two receptors in pathological situations, but the normal biological functions of DC-SIGNR are not well understood.

Previous structural studies on the CRDs of DC-SIGN and DC-SIGNR in complex with oligosaccharides have led to a proposed mechanism for selective binding of high-mannose oligosaccharides[14]. The purpose of the studies reported here is to elucidate the structural basis for binding of multiple types of glycan ligands to DC-SIGN and to define the distinct biochemical properties of DC-SIGN and DC-SIGNR in order to provide insight into their different biological roles.

RESULTS

DC-SIGN and DC-SIGNR binding to a glycan array

The recent demonstration that DC-SIGN binds to a selected set of fucosylated oligosaccharides, including Lewis^a and Lewis^x blood

[1]Glycobiology Institute, Department of Biochemistry, University of Oxford, Oxford OX1 3QU, UK. [2]Departments of Structural Biology and Molecular and Cellular Physiology, Stanford University School of Medicine, Stanford, California 94305, USA. [3]Department of Biochemistry & Molecular Biology, Protein-Carbohydrate Interaction Core H, Consortium for Functional Glycomics, University of Oklahoma Health Science Center, Oklahoma City, Oklahoma 73104, USA. [4]Department of Molecular Biology, Consortium for Functional Glycomics, Carbohydrate Synthesis and Protein Expression Core D, CB248, The Scripps Research Institute, 10550 North Torrey Pines Road, La Jolla, California 92037, USA. [5]These authors contributed equally to this work. Correspondence should be addressed to K.D. (kurt.drickamer@bioch.ox.ac.uk).

Published online 13 June 2004; doi:10.1038/nsmb784

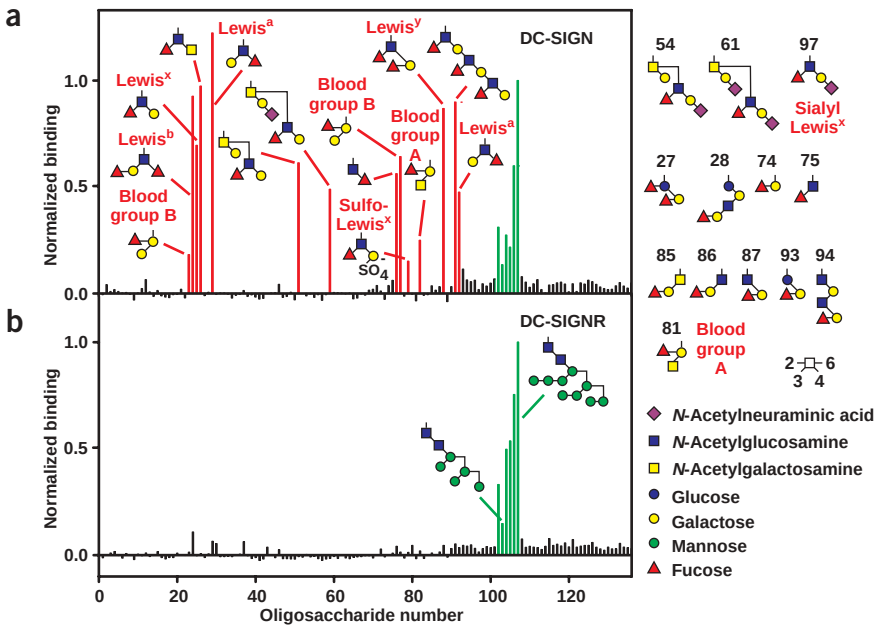

Figure 1 Glycan array probed with fluorescein-labeled DC-SIGN and DC-SIGNR. A complete listing of glycans is provided in **Supplementary Table 1** online. After subtraction of the background signal, the level of fluorescence for each protein (average of three wells) was normalized to the value for glycan 107 ($Man_9GlcNAc_2Asn$). Average s.d. of 10–12% were obtained for triplicates in a given assay and essentially identical results were produced in independent replicates. Fucose-containing ligands that do not bind are at right. Glycan 81 has the same oligosaccharide structure but a shorter spacer as compared with glycan 82, which binds weakly. Similarly, glycan 77, with an extended spacer, binds better than glycan 23. Linkages are α for all fucose and mannose residues and β in all other cases, except where indicated otherwise.

group epitopes found on some pathogens[14], suggested that a wider screen for potential ligands would be informative. The development of arrays of immobilized oligosaccharides provides a new way to undertake such screening and allows a broad comparison of the specificities of DC-SIGN and DC-SIGNR[15]. The array we used for these studies consists of biotinylated oligosaccharides immobilized in streptavidin-coated wells[16]. The primary array is populated with synthetic oligosaccharides created by a combination of chemical and enzymatic methods and linked to biotin through a spacer[17], as well as with some N- and O-linked glycan-amino acid conjugates derived from glycoproteins and linked to biotin through the amino group of the amino acid residue. The version of the array we used contained 19 monosaccharides, 33 disaccharides, 43 trisaccharides and 40 larger structures, including both neutral and acidic sugars containing either sialic acids or sulfate. It was probed with fluorescently labeled extracellular domains of DC-SIGN and DC-SIGNR, which form tetramers that can bind with enhanced avidity to glycans presented at high density on the surface of the wells[4].

The results of the initial screening of the array reveal that DC-SIGN and DC-SIGNR have markedly different ligand-binding characteristics (**Fig. 1**). Both receptors bind to N-linked high-mannose oligosaccharides. The highest level of binding was seen for a $Man_9GlcNAc_2Asn$ glycopeptide and binding decreased for smaller glycans in the series. The assays were conducted at a single concentration point and thus did not yield affinity values. However, the uniform concentration of streptavidin in the wells and the binding of biotinylated sugars at saturating concentrations mean that the relative fluorescence signals provide an accurate indication of the rank order of affinities. For example, the relative affinity for $Man_9GlcNAc_2$ was found to be more than seven-fold higher than the affinity for $Man_5GlcNAc_2$; this is consistent with the results of solution-phase competition assays[14].

The mannose-containing glycans are the only ligands in the array that are bound above background levels by DC-SIGNR. In contrast, 14 other glycans react with DC-SIGN. All of these glycans contain terminal fucose residues, but these are linked to various different hydroxyl groups on several different underlying sugar residues. These ligands include structures that form blood group substances in addition to Lewis^x and Lewis^a epitopes, consistent with previous findings[11]. An additional 13 glycans in the array have terminal fucose residues but do not bind DC-SIGN, indicating that the presence of a terminal fucose residue is not the sole determinant of binding to these ligands. Comparison of the structures of the ligands that bind with those that do not bind reveals three distinct features. First, all but one of the ligands that do bind contain branched terminal structures, so that the fucose is always linked to an underlying sugar at a hydroxyl group adjacent to a galactose or *N*-acetylgalactosamine residue. All of these glycans have the potential to assume compact configurations in which the hydrophobic B faces of galactose (or *N*-acetylgalactosamine) and fucose pack against each other, as they do in Lewis^x and Lewis^a trisaccharides. The only linear oligosaccharide that binds to DC-SIGN is Fucα1-4GlcNAc, which is also the only linear structure in which fucose is linked to GlcNAc, showing that the GlcNAc enhances binding to the CRD, although it may do so in a manner different than that of the other glycans. A second phenomenon is that several branched ligands containing the Lewis^x trisaccharide sialylated on the 3 position of galactose do not bind, as has been noted in previous studies[11]. These results indicate that the presence of the bulky and charged sialic acid residue prevents binding. The 3-sulfated form of Lewis^x binds weakly, suggesting that the sulfate residue causes partial exclusion. Finally, although the trisaccharide of blood group A binds to DC-SIGN (compound 82) when presented on the usual spacer arm, a version with a shorter spacer (compound 81) does not bind. This result emphasizes that the extent of binding can be substantially influenced by the way the glycan is presented.

Similar results were observed with multivalent glycosylated polyacrylamide derivatives that were tested in the same array format. Although both DC-SIGN and DC-SIGNR bind to the polyvalent ligand that has a tri-mannose structure, only DC-SIGN binds detectably to the fucose-containing polymer (**Supplementary Fig. 1** online).

Structures of ligand complexes

Previous structural studies of DC-SIGN and DC-SIGNR bound to an oligosaccharide have suggested a mechanism for the binding of high-mannose oligosaccharides[14], but our array screening results indicated the need for further structural analysis to explain the different characteristics of the two proteins and the apparent dual specificity of DC-SIGN for two classes of ligands. We obtained insight into the ability of DC-SIGN to bind fucosylated ligands from crystals of the CRD of

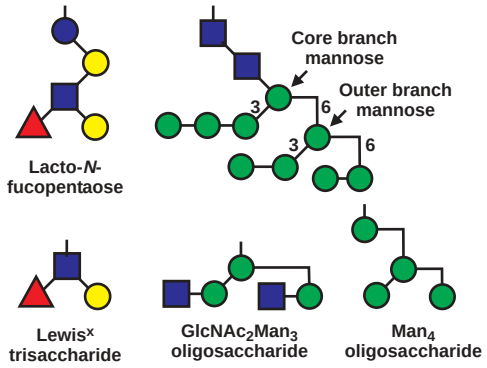

Figure 2 Oligosaccharides used in structural studies of DC-SIGN and DC-SIGNR. Symbols are as defined in **Figure 1**. Structures of the complexes of both proteins with the GlcNAc$_2$Man$_3$ oligosaccharide are as described[14]. This oligosaccharide contains a branch mannose that is not linked to other sugars. The branch mannose residues in the high-mannose oligosaccharide are linked in either α (outer branch) or β (core branch) configuration. The Man$_4$ oligosaccharide is an analog of the outer branch structure.

DC-SIGN bound to the pentasaccharide lacto-*N*-fucopentaose III (LNFP III), which contains the Lewis^x trisaccharide (**Fig. 2**). The primary carbohydrate-binding site of C-type lectins comprises a conserved Ca^{2+}, designated the principal Ca^{2+} site, which is coordinated by adjacent OH groups of the pyranose ring[18]. In the LNFP III complex, the 3- and 4-OH groups of the α1-3-linked fucose residue form these coordination bonds (**Fig. 3a**,**b**). Because the 3-OH group is equatorial and the 4-OH group is axial, the sugar is tipped compared with the way that mannose, with equatorial 3- and 4-OH groups, is bound in the primary binding site (**Fig. 3c**,**d**). This orientation positions the fucose ring close to Val351, which forms tight van der Waals contacts with the 2-OH group. The compact structure of the Lewis^x trisaccharide is oriented with the central GlcNAc residue pointing away from the protein and the terminal galactose residue contacting the protein in a secondary binding site (**Fig. 3b**). Asp367 forms part of a hydrogen-bond network, bridging the distance between Lys373 and the 6-OH group of the galactose, whereas Leu371 makes van der Waals contacts with this same portion of the sugar. An additional network of hydrogen bonds links Lys373 with Glu358, which in turn hydrogen-bonds to the 4-OH group of galactose through a water molecule. Additional water-mediated hydrogen bonds connect Asp367 and Lys368 with the fucose and GlcNAc residues.

The orientation of the Lewis^x trisaccharide in the binding site of DC-SIGN suggests that other fucose-containing ligands probably bind with fucose in the primary binding site, although they may make somewhat different contacts with the secondary binding site. The extra fucose residue linked to the 2-OH group of galactose in the Lewis^y oligosaccharide would be positioned away from the protein and thus would not interfere with binding. The finding that sulfation of Lewis^a does not completely block binding suggests that this oligosaccharide is shifted somewhat in the binding site. The structure also explains the absence of binding to ligands in which the Lewis^x determinant is extended. For example, the observation that 3′ sialylation or sulfation of Lewis^x abrogates binding to DC-SIGN can be explained by the fact that a substituent on the 3-OH group of galactose would clash with Phe313.

Crystals of a fragment of DC-SIGNR were also obtained in the presence of the simple Lewis^x trisaccharide. The DC-SIGNR fragment contains a portion of the neck in addition to the CRD, which will be the subject of a separate communication (H.F., Y.G., K.D. and W.I.W., unpublished data). The fact that DC-SIGNR has only weak affinity for this ligand explains the poor definition of the sugar density; this probably results from partial occupancy of the site even at the concentration (10 mM) used in the crystallization. The position of the bound trisaccharide is very similar to the position of the corresponding portion of the LNFP III ligand in the DC-SIGN binding site (**Fig. 4a**,**b**). An important difference in the primary binding site is the replacement of Val351 of DC-SIGN with Ser363 in DC-SIGNR, eliminating the van der Waals interaction with the 2-OH group of fucose. In addition, certain contacts in the secondary binding site are different owing to a slight shift in orientation of the ligand that arises from differences in the amino acid sequences. For example, the distance between the 6-OH of galactose and Asn379 (>3.4 Å) is longer than the corresponding distance to Asp367 in DC-SIGN (2.6 Å), in part because Asn385 in DC-SIGNR, which corresponds to Lys373 in DC-SIGN, does not interact with Asn379.

On the basis of the crystal structures of DC-SIGN and DC-SIGNR with the pentasaccharide GlcNAc$_2$Man$_3$, it has been previously suggested that binding of *N*-linked high-mannose oligosaccharides

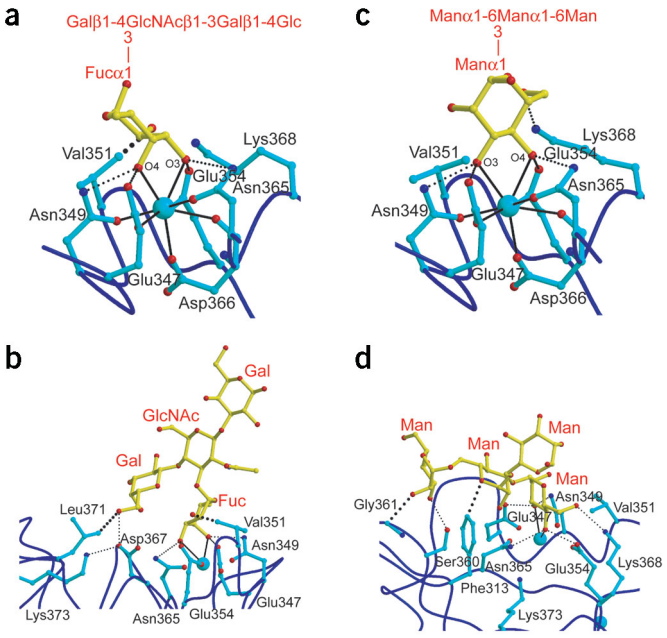

Figure 3 DC-SIGN interactions with fucosylated and high-mannose oligosaccharides. (**a**) Close-up view of the fucose residue of LNFP III in the primary binding site. (**b**) Structure of LNFP III bound to DC-SIGN. (**c**) Close-up of the terminal, nonreducing α1-3-linked mannose of the Man$_4$ structure in the primary site. The 6-OH group is within hydrogen bond distance of one of the two conformations of the side chain of Lys368. (**d**) Structure of Man$_4$ bound to DC-SIGN. Gly361 makes van der Waals contact with the terminal, nonreducing α1-6 linked mannose residue and Glu358 (not shown) indirectly forms hydrogen bonds to the branch mannose through water molecules. The views in **b** and **d** are rotated ~180° about the vertical relative to those in **a** and **c**. The protein backbone is blue, and bonds are cyan. Bonds in the carbohydrate are yellow. Carbon, nitrogen, oxygen and Ca^{2+} are cyan, blue, red and large cyan spheres, respectively. Ca^{2+} coordination bonds are solid lines, hydrogen bonds are thin dotted lines and van der Waals contacts are thick dotted lines.

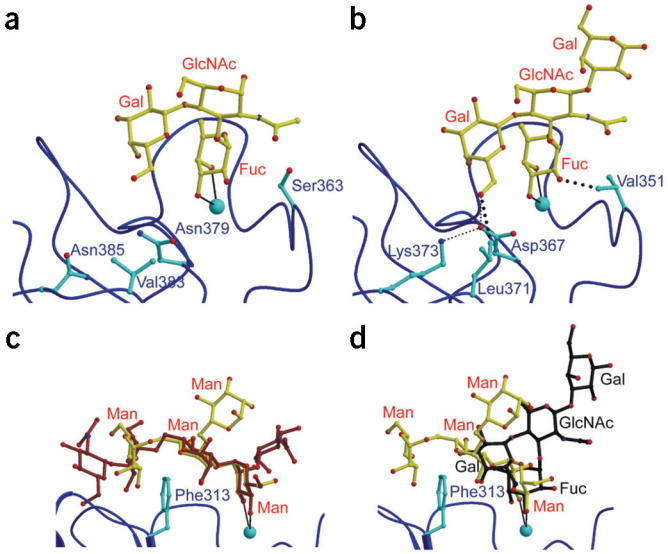

Figure 4 DC-SIGN and DC-SIGNR interactions with Lewis^x and oligomannosides. (**a**) DC-SIGNR bound to Lewis^x trisaccharide. (**b**) DC-SIGN bound to LNFP III. In **a** and **b**, key residues that differ between DC-SIGN and DC-SIGNR are shown. (**c**) Comparison of Man_4 (yellow bonds) binding with $GlcNAc_2Man_3$ (red bonds)[14]. Phe313 interacts with the Manα1-6Man moiety of the trimannose structure. (**d**) Comparison of Man_4 (yellow bonds) and LNFP III (black bonds) bound to DC-SIGN. The color scheme is the same as in **Figure 3**.

involves a more extended secondary binding site than that observed for Lewis^x-containing ligands[14]. Both receptors recognize the branched trimannose structure Manα1-3(Manα1-6)Manα1-. Phe313 has been postulated to play two roles in selective binding of high-mannose glycans: increasing affinity by forming part of a surface complementary to the shape of the Manα1-6Man moiety (**Fig. 4c**), and allowing access to the α-linked outer arm branch trimannose while excluding the β-linked core branch trimannose. In this way, Phe313 would prevent the binding of complex *N*-linked glycans that have only the core branch trimannose structure, while accommodating high-mannose oligosaccharides by binding to the outer branched trimannose. This proposal was tested by examining the structure of the CRD of DC-SIGN bound to a Man_4 oligosaccharide in which the branched trimannose is in an α linkage (**Fig. 4c**). Compared with the previously reported structure, the conformations of the Man_3 moieties common to both oligosaccharides are similar and form van der Waals contacts with Phe313 and hydrogen bonds with Ser360 in the secondary binding site. In the primary binding site, Val351 is 3.9 Å away from the mannose residue and thus does not contribute van der Waals interactions as it does for fucose. As proposed, the α-linked reducing mannose residue is accommodated because it points away from the protein, thereby permitting binding of high-mannose oligosaccharides[14].

Mutagenesis of binding site residues

Relative affinities derived from competition experiments demonstrate preferential binding of fucose to DC-SIGN and mannose to DC-SIGNR (**Table 1**). The key difference in the primary binding site is the presence of van der Waals contacts between the 2-OH of bound fucose and Val351 in DC-SIGN; no such contact is made with the corresponding residue in DC-SIGNR, Ser363. Substitution of serine or alanine for Val351 in DC-SIGN leads to an inversion of selectivity, with mannose becoming the preferred ligand. Conversely, replacement of Ser363 in DC-SIGNR with valine increases the affinity for fucose compared with that of the wild type protein. These results provide strong evidence that the van der Waals interaction between Val351 and fucose is the main factor determining differential monosaccharide binding at the primary binding site of DC-SIGN.

The importance of the primary binding site selectivity in determining specificity for oligosaccharide ligands was demonstrated using an assay format exactly analogous to the array screen (**Fig. 5**). The V351S mutation substantially reduced binding to the fucosylated oligosaccharides relative to the high mannose structure, whereas a V351A substitution had a less marked effect. In DC-SIGNR, the S363V substitution had the opposite effect: Lewis^a and Lewis^x glycans, which bind very poorly to wild-type DC-SIGNR, bind to the S363V mutant almost as well as the Man_9 ligand. These results support the proposal that enhanced binding of fucose at the primary binding site is the predominant factor in generating the broader ligand-binding profile of DC-SIGN. However, in addition to reducing the affinity for fucose-containing ligands by eliminating a key van der Waals contact in the primary binding site, serine at this position probably enhances binding to the high-mannose oligosaccharide by making a hydrogen bond to the α1,2-linked mannose residue on the 3′ branch, as it does with the terminal GlcNAc residue of the $Man_3GlcNAc_2$ oligosaccharide in the previously described crystal structure[14].

The contributions of the interactions with fucosylated ligands observed at the secondary site were also investigated by mutagenesis.

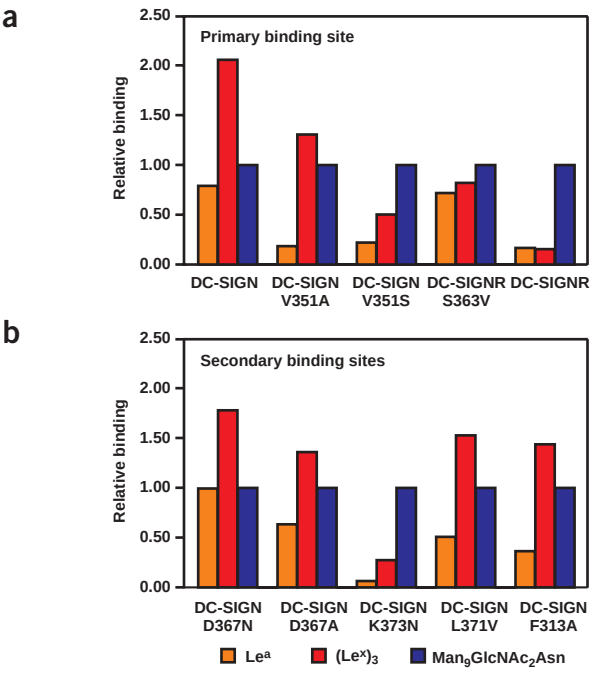

Figure 5 Binding of mutant DC-SIGN and DC-SIGNR to selected glycans. Binding of ^{125}I-labeled extracellular domains to biotinylated oligosaccharides immobilized on streptavidin-coated plates was normalized to the binding seen for $Man_9GlcNAc_2Asn$. Results are averages of three experiments, each done in duplicate.

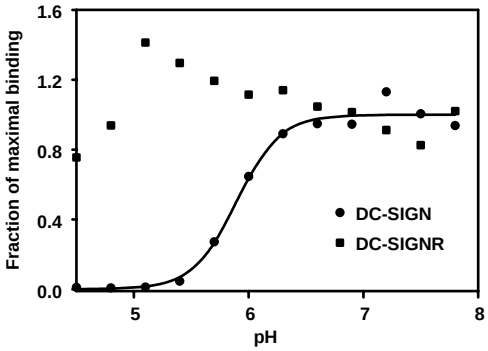

Figure 6 pH-dependence of ^{125}I-labeled Man_{30}-BSA binding to immobilized DC-SIGN and DC-SIGNR. Binding was normalized to the binding in the plateau region >pH 6.5. The results for DC-SIGN were fitted to a curve for pH-dependence[19], but the results for DC-SIGNR could not be fitted to any simple binding equation. The results are representative of six similar experiments.

These mutations have little effect on the relative affinities for the monosaccharides mannose and fucose, as these affinities are determined by residues in the primary binding site (**Table 1**). The importance of the hydrogen-bonding network that includes Lys373, Asp367 and the 6-OH group of the terminal galactose residue in Lewis^x was investigated by changing these residues to their equivalents in DC-SIGNR. The D367N substitution had essentially no effect on the relative binding of fucose- and mannose-containing oligosaccharides. The side chain of asparagine would be able to mimic aspartic acid and participate in the same hydrogen-bonding network, bridging the amino group of Lys373 and the 6-OH of galactose, although this would require rotation of the asparagine side chain compared with the orientation seen in DC-SIGNR. A D367A substitution substantially reduced the relative affinity for both Lewis^a and Lewis^x oligosaccharides, reflecting the loss of the hydrogen bond to galactose. More markedly, the K373N mutation almost completely converted the ligand-binding characteristics of DC-SIGN to those of DC-SIGNR, showing that Lys373 plays a critical part in the interactions at the secondary binding site. The extreme phenotype of the K373N mutant reflects the fact that, in addition to making a hydrogen bond to Asp367, Lys373 also interacts indirectly through water and the side chain of Glu358 with the 4-OH group of galactose. Changing Leu371 to a valine, which is found at position 389 of DC-SIGNR, had an effect similar to the D367A mutation, confirming the importance of the van der Waals packing of this residue against the 6-OH of galactose.

An important feature of the secondary binding site is the exclusion of Lewis^x derivatives that contain a large sialic acid substituent on the galactose residue. Although the bulky side chain of Phe313 is a potential factor in preventing binding of sialylated ligands (**Fig. 4d**), probing of sialylated Lewis^x oligosaccharides with wild-type and F313A mutant DC-SIGN revealed no detectable binding to either protein (data not shown). Thus, although a steric clash with Phe313 may contribute to the exclusion of sialylated ligands, other factors such as electrostatic repulsion must also play a role. Several of the mutations in the secondary binding site differentially affect binding of Lewis^a and Lewis^x ligands, suggesting that the galactose moiety of the Lewis^a trisaccharide in the binding site occupies a slightly different position than the galactose of the Lewis^x trisaccharide.

Distinct trafficking of DC-SIGN and DC-SIGNR

The ability of DC-SIGN to mediate uptake of viruses and microorganisms suggests that it might behave as a recycling receptor. An important property of such receptors is their ability to release ligands at low pH, which allows segregation of ligands from the receptors in endosomes. When analyzed at physiological Ca^{2+} concentration, the pH for half-maximal binding of ligand to the extracellular domain of DC-SIGN is 5.91 ± 0.02 (**Fig. 6**). In this respect, DC-SIGN is similar to well-characterized endocytic receptors containing C-type CRDs, such as the asialoglycoprotein receptor[19]. Titration of key side chains in the CRD of the asialoglycoprotein receptor leads to structural alterations in the primary Ca^{2+} site, thereby compromising the receptor's ability to bind Ca^{2+} and saccharide ligands. Similar experiments with DC-SIGNR failed to show decreased ligand binding compared with binding at neutral pH even at pH values <5. These results are consistent with sugar specificity data showing that although DC-SIGN and DC-SIGNR are closely related, their binding sites have evolved to serve different functions.

The failure of DC-SIGNR to release ligands at pH values such as those found in endosomes indicated that it might not function as a recycling endocytic receptor. We tested this possibility by examining cells expressing the full-length receptors (**Fig. 7**). The results reveal that DC-SIGN and DC-SIGNR have distinctly different properties. Neoglycoprotein ligand bound to DC-SIGN is efficiently internalized and degraded. The rate of ligand processing is consistent with receptor recycling, as the number of molecules processed per cell over a 2-h period is roughly tenfold higher than the estimated level of receptor expression. In contrast, no pool of internalized neoglycoprotein was detected in cells expressing DC-SIGNR and no degradation was observed. Immunoblotting experiments confirmed that the two proteins are present at comparable levels (data not shown) and immunofluorescence demonstrated that both are expressed at the cell surface (**Fig. 7**).

Two types of sequences in the cytoplasmic tail of DC-SIGN have been proposed to direct localization in endocytic vesicles[20]. The di-leucine motif is conserved in the tail of DC-SIGNR, but the YXXΦ (where X is any residue and Φ is a hydrophobic residue) motif is not.

Table 1 Mutant DC-SIGN and DC-SIGNR binding to saccharide ligands

Protein	$K_{i,Fuc}/K_{i,Man}$[a]	B_{Man9}/B_{LeX3}[b]
Wild-type proteins		
DC-SIGN	0.61 ± 0.09	0.48 ± 0.03
DC-SIGNR	1.69 ± 0.27	6.67 ± 0.67
Primary binding site mutations		
DC-SIGN V351A	1.05 ± 0.11	0.81 ± 0.05
DC-SIGN V351S	1.33 ± 0.12	2.00 ± 0.04
DC-SIGNR S363V	1.05 ± 0.12	1.26 ± 0.02
Secondary binding site mutations		
DC-SIGN D367N	0.59 ± 0.24	0.56 ± 0.01
DC-SIGN D367A	0.58 ± 0.06	0.79 ± 0.01
DC-SIGN K373N	0.79 ± 0.14	4.00 ± 0.50
DC-SIGN L371V	0.72 ± 0.21	0.65 ± 0.02
DC-SIGN F313A	0.56 ± 0.04	0.68 ± 0.02

[a]Relative inhibition constants for monosaccharides (K_i) were determined in binding competition assays in which the reporter ligand ^{125}I-labeled Man_{30}-BSA was bound to CRDs immobilized in polystyrene wells. [b]Relative binding to oligosaccharides (B) was quantified from **Figure 5**.

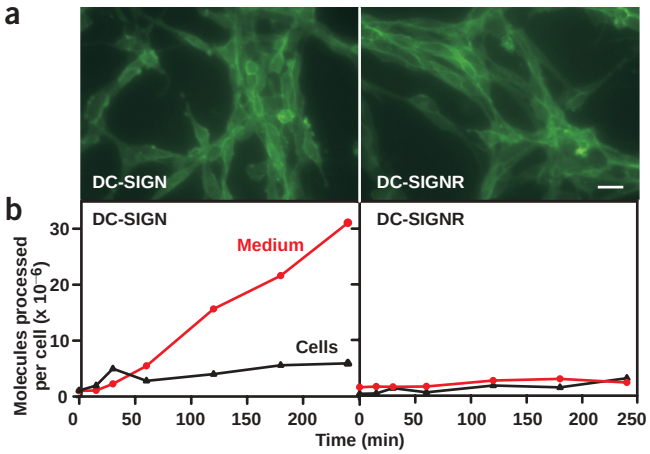

Figure 7 Uptake and degradation of ^{125}I-labeled Man_{30}-BSA by cells expressing DC-SIGN and DC-SIGNR. (**a**) Surface expression is documented by staining of unpermeabilized cells with fluorescein-labeled antibodies. Scale bar, 20 μm. (**b**) Cell-associated radioactivity and acid-soluble degradation products released back into the medium were quantified after incubation for the indicated times at 37 °C. The results are representative of three similar experiments.

Although previous experiments have suggested that the di-leucine motif is necessary for endocytic function of DC-SIGN[20], it seems that this signal is not sufficient to direct internalization of DC-SIGNR. Thus, both the extracellular and cytoplasmic portions of DC-SIGN have evolved in comparison to DC-SIGNR so that DC-SIGN can mediate multiple ligand-binding and intracellular trafficking functions.

DISCUSSION

The dual specificity of DC-SIGN indicates that this receptor has evolved to recognize specific classes of glycans that are expressed on mammalian glycoproteins, but that also appear on certain pathogens. Binding to DC-SIGN through high-mannose-type glycans is exploited by some viruses, notably HIV, but such interactions may participate in generating protective immune responses for other viruses that bear such sugar structures. Thus, selective recognition of this class of oligosaccharides would be relevant to defense against viral pathogens. Similarly, the fucose-containing oligosaccharides bound most effectively by DC-SIGN can be endogenous structures, but also appear on parasites that bind DC-SIGN[11]. The key to selective interaction with pathogens may be in the binding of closely spaced glycans by the multiple CRDs in the DC-SIGN tetramer, because clusters of either mannose-type or fucose-type ligands are uncommon on endogenous cell surfaces and glycoproteins.

The mechanisms of glycan binding to DC-SIGN can be contrasted with the binding of ligands to other sugar-selective adhesion and pathogen receptors. The selectins bind sialylated forms of the Lewis[a] and Lewis[x] trisaccharides, with fucose binding in the primary binding site and galactose and the appended sialic acid binding to a secondary site. The orientation of fucose in the primary binding site of E- and P-selectins is very similar to that in the DC-SIGN site. The secondary site is in the same general area as the secondary binding sites in DC-SIGN, including residues of E-selectin that correspond to residues 358 and 360 in DC-SIGN and a long inserted loop that forms an extended secondary binding site as compared with that of DC-SIGN.

Pathogen receptors such as serum mannose-binding protein and the macrophage mannose receptor bind to ligands bearing terminal fucose, mannose or GlcNAc with broad specificity by interacting with these monosaccharides in terminal positions on many types of glycans, through the primary binding site only[21]. Mannose-binding protein binds to the 2- and 3-OH groups of fucose, rather than to the 3- and 4-OH groups as in DC-SIGN[22]; this orients fucose like mannose, leading to an absence of secondary binding site interactions. In contrast, dual specificity for mannose- and fucose-containing ligands exhibited by DC-SIGN arises from the distinct binding geometry of mannose and fucose in the primary site, which permits formation of favorable contacts in distinct secondary binding sites for these classes of oligosaccharides. The fact that different sugars have different secondary binding sites in DC-SIGN suggests that it may be possible to design inhibitors that selectively inhibit binding to only one subset of ligands.

METHODS

Carbohydrate binding assays. Extracellular domain fragments of wild-type and mutant DC-SIGN and DC-SIGNR were dialyzed into 150 mM NaCl containing 100 mM Na-HEPES, pH 7.8, and 10 mM $CaCl_2$, and reacted with fluorescein isothiocyanate (50 μg mg protein^{-1}) or ^{125}I-Bolton-Hunter reagent (50 μCi mg protein^{-1}). Procedures for probing the full glycan arrays are available at http://web.mit.edu/glycomics/consortium. Biotinylated glycans obtained from the Consortium for Functional Glycomics, Dextra Laboratories, and by reaction of the glycopeptide from soybean agglutinin[4] with LC-biotin (Pierce Chemical), were bound to streptavidin-coated plates (Pierce Chemical) by incubation overnight at 4 °C at a concentration of 100 μM. Radio-iodinated proteins were incubated in the wells for 2 h at 4 °C in a buffer containing 150 mM NaCl, 25 mM Tris-Cl, pH 7.8, 25 mM $CaCl_2$ and 0.1 mg ml^{-1} BSA and washed three times in the same buffer, without added albumin, before counting of radioactivity.

Table 2 Crystallographic data and refinement statistics

	DC-SIGN CRD + Man_4	DC-SIGN CRD + LNFP III	DCSIGN-R dimer + Lewis[x]
Data collection			
Space group	$P4_3$	$P2_12_12$	$P3_221$
Unit cell dimensions (Å)			
a	55.7	72.6	153.8
b	–	55.4	–
c	53.3	29.6	128.7
Resolution (Å)[a]	53.3–1.55 (1.59–1.55)	43.8–1.8 (1.86–1.8)	41.9–2.25 (2.33–2.25)
R_{sym}[a]	6.2 (23.9)	5.9 (27.8)	5.4 (32.2)
Completeness (%)[a]	100 (99.8)	96.5 (91.4)	96.5 (84.5)
Average multiplicity	9.9	6.7	4.4
Refinement			
R_{free}	25.5	22.3	25.6
R	22.3	17.9	21.9
Average *B*-factor (Å^2)	24.1	18.4	54.1
R.m.s. deviations			
Bond length (Å)	0.0048	0.0046	0.0060
Bond angle (°)	1.24	1.24	1.18

[a]Values in parentheses are for the highest-resolution shell.

Characterization of mutant receptors. Mutations were introduced into cDNAs for DC-SIGN and DC-SIGNR by using synthetic DNA restriction fragments to replace the wild-type sequences[23]. Extracellular domain and CRD fragments were expressed and purified as for the wild-type proteins[4]. Inhibitory activity of monosaccharides[4] and pH-dependence of binding[19] were assayed using CRDs immobilized in polystyrene wells. Buffers for the pH assays contained 25 mM MOPS and 25 mM MES.

Analysis of transfected fibroblasts. Retroviral vectors containing cDNAs for full length DC-SIGN and DC-SIGNR were introduced into a packaging cell line to produce pseudo viruses that were used to infect Rat-6 fibroblasts. Cell lines stably expressing DC-SIGN or DC-SIGNR were selected with G418 (ref. 24). Endocytosis assays were conducted as described for similar cell lines expressing other C-type lectins[25]. Antibodies to DC-SIGN and DC-SIGNR were produced in rabbits using the CRD fragments as immunogens and were affinity-purified on Affigel-10 columns (BioRad Laboratories) conjugated with the corresponding extracellular domain fragments. Cells grown on glass coverslips were fixed with paraformaldehyde[26] and stained with antibody that was labeled with fluorescein using the Xenon labeling kit from Molecular Probes.

Crystallization and structure determination. Crystals were grown at 21 °C using the hanging-drop method (0.9 or 1 μl protein to 0.9 or 1 μl reservoir). The protein solution contained 10 mg ml^{-1} protein, 5 mM $CaCl_2$ and 10 mM oligosaccharides (obtained from Dextra Laboratories). For the DC-SIGN CRD–Man_4 complex, the reservoir solution contained 20% (w/v) polyethylene glycol PEG 400 and 0.1 M Tris-Cl, pH 7.0, and crystals were frozen directly from the drop in liquid nitrogen. For the DC-SIGN CRD–LNFP III complex, the reservoir solution contained 30% (w/v) PEG 4000, 0.2 M $MgCl_2$ and 0.1 M Tris-Cl, pH 8.5. These crystals were transferred to 30% (w/v) PEG 4000, 0.2 M $MgCl_2$, 0.1 M Tris-Cl, pH 8.5, 5 mM $CaCl_2$ and 10 mM oligosaccharide for freezing. Crystals of the dimeric DC-SIGNR bound to $Lewis^x$ trisaccharide were prepared with a reservoir solution containing 30% (w/v) PEG 300, 0.2 M NaCl and 0.1 M HEPES, pH 7.5; the crystals were frozen directly from the drop. All crystals were maintained at 100 K during data collection.

Diffraction data were measured on the Advanced Light Source beamlines 8.3.1 (DC-SIGN CRD + Man_4) and 8.2.2 (DC-SIGN CRD + LNFP III and DCSIGN-R dimer + $Lewis^x$) on ADSC Q315 CCD detectors, and processed with MOSFLM[27] and SCALA[28] (Man_4 complex) or DENZO and SCALEPACK[29] (LNFP III and Le^x complexes) (**Table 2**). All structures were determined by molecular replacement. Refinement and map calculations were carried out using CNS[30]. Bulk solvent and anisotropic temperature factor corrections were applied during the refinement. The resolution was gradually increased to the maximum resolution using the MLF target. Water molecules were added to peaks >3 σ in $F_o - F_c$ maps and were within hydrogen bond distance to the protein or other water molecules. The final electron density maps near the carbohydrate-binding sites are shown in **Supplementary Figure 2** online.

Molecular replacement phasing of the DC-SIGN–Man_4 complex was carried out with COMO[31], using the DC-SIGN CRD (PDB entry 1K9I) as a search model. The best solution had a correlation coefficient of 48.2% and *R*-factor of 44.7% (resolution range 15–3.0 Å). The final model contains residues 253–384, one molecule of Man_4 and 152 water molecules. On the Ramachandran plot, 91.4%, 7.7%, 0.9% and 0% of the residues are found in the most favored, allowed, generously allowed and disallowed regions, respectively. Molecular replacement phasing of the LNFPIII–DC-SIGN CRD complex was performed with AmoRe[32] using the CRD from the Man_4 complex as a search model. The best solution had a correlation coefficient of 41.3% and an *R*-factor of 36.2% for data to 3.0 Å. On the basis of bond distances and temperature factors, one of the two metals occupying the auxiliary metal binding site was assigned as Mg^{2+}. The final model contains residues 253–383, four of the five sugar residues of LNFP III (the $Lewis^x$ portion of the sugar and the reducing end galactose), two Ca^{2+}, one Mg^{2+}, and 192 water molecules. On the Ramachandran plot, 88.7%, 9.6%, 1.7% and 0% of the residues are found in the most favored, allowed, generously allowed and disallowed regions. The asymmetric unit of the $Lewis^x$-DC-SIGNR crystals contains six copies, each comprising a CRD and dimerization domain (three dimers per asymmetric unit). A solution for the CRDs of one dimer was found using CNS[30], with the CRD structure (PDB entry 1K9J) as a search model. The CRDs for the three dimers in the asymmetric unit were then found with COMO[31], using the dimer solution from CNS as the search model. The best solution had a correlation coefficient of 34.9% and an *R*-factor of 43.1% (resolution range 13–3.5 Å). Strict three-fold noncrystallographic symmetry was imposed in the initial stages of refinement, but was later removed, leading to lower R_{free} values. After several rounds of refinement, most of the dimerization domain could be added to the model. A strong peak in the map, in close proximity to four oxygen atoms in the dimerization domain, was assigned as Ca^{2+}. The final model consists of residues 219–234 and 246–397 for copies A, B and C, residues 219–237 and 249–397 for copies D, E and F, 6 $Lewis^x$ molecules, 24 Ca^{2+} and 236 water molecules. On the Ramachandran plot, 89.1%, 10.6%, 0.3% and 0% of the residues are found in the most favored, allowed, generously allowed and disallowed regions.

Coordinates. Coordinates and structure factors for the Man_4, LNFPIII and $Lewis^x$ complexes have been deposited in the Protein Data Bank (accession codes 1SL4, 1SL5 and 1SL6, respectively).

Note: Supplementary information is available on the Nature Structural & Molecular Biology website.

ACKNOWLEDGMENTS

We thank D. Torgersen for help with protein preparation and P. Lee for glycan array analysis. This work was supported by Wellcome Trust grant 041845 to K.D., a grant from the Mizutani Foundation for Glycoscience to W.I.W. and US National Institutes of Health grants GM50565 to W.I.W. and GM62116 to the Consortium for Functional Glycomics. Diffraction data were measured at the Advanced Light Source of the Lawrence Berkeley National Laboratory.

COMPETING INTERESTS STATEMENT

The authors declare that they have no competing financial interests.

Received 23 February; accepted 15 April 2004
Published online at http://www.nature.com/nsmb/

1. Steinman, R.M. DC-SIGN: a guide to some mysteries of dendritic cells. *Cell* **100**, 491–494 (2000).
2. Cambi, A.C. & Figdor, C.G. Dual function of C-type lectin-like receptors in the immune system. *Curr. Opin. Cell Biol.* **15**, 539–546 (2003).
3. Geijtenbeek, T.B.H. *et al.* Identification of DC-SIGN, a novel dendritic cell-specific ICAM-3 receptor that support primary immune responses. *Cell* **100**, 575–585 (2000).
4. Mitchell, D.A., Fadden, A.J. & Drickamer, K. A novel mechanism of carbohydrate recognition by the C-type lectins DC-SIGN and DC-SIGNR: subunit organisation and binding to multivalent ligands. *J. Biol. Chem.* **276**, 28939–28945 (2001).
5. van Kooyk, Y., Appelmelk, B. & Geijtenbeek, T.B.H. A fatal attraction: *Mycobacterium tuberculosis* and HIV-1 target DC-SIGN to escape immune surveillance. *Trends Mol. Med.* **9**, 153–159 (2003).
6. van Kooyk, Y. & Geijtenbeek, T.B.H. DC-SIGN: escape mechanism for pathogens. *Nat. Rev. Immunol.* **3**, 697–709 (2003).
7. Pöhlmann, S., Baribaud, F. & Doms, R.W. DC-SIGN and DC-SIGNR: helping hands for HIV. *Trends Immunol.* **22**, 643–646 (2001).
8. Alvarez, C.P. *et al.* C-types lectins DC-SIGN and L-SIGN mediate cellular entry by Ebola virus in cis and trans. *J. Virol.* **76**, 6841–6844 (2002).
9. Simmons, G. *et al.* DC-SIGN and DC-SIGNR bind Ebola glycoproteins and enhance infection of macrophages and endothelial cells. *Virology* **305**, 115–123 (2003).
10. Frison, N. *et al.* Oligolysine-based oligosaccharide clusters: selective recognition and endocytosis by the mannose receptor and DC-SIGN. *J. Biol. Chem.* **278**, 23922–23929 (2003).
11. Appelmelk, B.J. *et al.* Carbohydrate profiling identifies new pathogens that interact with dendritic cell-specific ICAM-3-grabbing nonintegrin on dendritic cells. *J. Immunol.* **170**, 1635–1639 (2003).
12. Cambi, A. *et al.* The C-type lectin DC-SIGN (CD209) is an antigen-uptake receptor for *Candida albicans* on dendritic cells. *Eur. J. Immunol.* **33**, 532–538 (2003).
13. Soilleux, E.J. DC-SIGN (dendritic cell-specific ICAM-grabbing non-integrin) and DC-SIGN-related (DC-SIGNR): friend or foe? *Clinical Sci.* **104**, 437–446 (2003).
14. Feinberg, H., Mitchell, D.A., Drickamer, K. & Weis, W.I. Structural basis for selective recognition of oligosaccharides by DC-SIGN and DC-SIGNR. *Science* **294**, 2163–2166 (2001).
15. Drickamer, K. & Taylor, M.E. Glycan arrays for functional genomics. *Genome Biol.* **3**, 1034.1–1034.4 (2002).
16. Leppanen, A., White, S.P., Helin, J., McEver, R.P. & Cummings, R.D. Binding of glycosulfopeptides to P-selectin requires stereospecific contributions of individual tyrosine sulfate and sugar residues. *J. Biol. Chem.* **275**, 39569–39578 (2000).

17. Blixt, O., Collins, B.E., van den Nieuwenhof, I.M., Crocker, P.R. & Paulson, J.C. Sialoside specificity of the siglec family assessed using novel multivalent probes: identification of potent inhibitors of myelin-associated glycoprotein. *J. Biol. Chem.* **278**, 31007–310019 (2003).
18. Drickamer, K. C-Type lectin-like domains. *Curr. Opin. Struct. Biol.* **9**, 585–590 (1999).
19. Wragg, S. & Drickamer, K. Identification of amino acid residues that determine pH-sensitivity of ligand binding to the asialoglycoprotein receptor. *J. Biol. Chem.* **274**, 35400–35406 (1999).
20. Engering, A. *et al.* The dendritic cell-specific adhesion receptor DC-SIGN internalizes antigen for presentation to T cells. *J. Immunol.* **168**, 2118–2126 (2002).
21. Weis, W.I., Taylor, M.E. & Drickamer, K. The C-type lectin superfamily in the immune system. *Immunol. Rev.* **163**, 19–34 (1998).
22. Ng, K.K.-S., Drickamer, K. & Weis, W.I. Structural analysis of monosaccharide recognition by rat liver mannose-binding protein. *J. Biol. Chem.* **271**, 663–674 (1996).
23. Maniatis, T., Fritsch, E.F. & Sambrook, J. *Molecular Cloning: A Laboratory Manual* (Cold Spring Harbor Laboratory Press, Cold Spring Harbor, New York, 1982).
24. Stambach, N.S. & Taylor, M.E. Characterization of carbohydrate recognition by langerin, a C-type lectin of Langerhans cell. *Glycobiology* **13**, 401–410 (2003).
25. Mellow, T.E., Halberg, D. & Drickamer, K. Endocytosis of *N*-acetylglucosamine-containing glycoproteins by rat fibroblasts expressing a single species of chicken liver glycoprotein receptor. *J. Biol. Chem.* **263**, 5468–5473 (1988).
26. Harlow, E. & Lane, D. *Antibodies: A Laboratory Manual* (Cold Spring Harbor Laboratory Press, Cold Spring Harbor, New York, 1988).
27. Leslie, A.G.W. In *Proceedings of the CCP4 Study Weekend: 'Data Collection and Processing'* (eds. Sawyer, L., Isaacs, N. & Bailey, S.) 44–51 (SERC Daresbury Laboratory, Daresbury, UK, 1993).
28. Collaborative Computational Project. The CCP4 suite: programs for protein crystallography. *Acta Crystallogr. D* **50**, 760–763 (1994).
29. Otwinowski, Z. & Minor, W. Processing of X-ray diffraction data collected in oscillation mode. *Methods Enzymol.* **276**, 307–326 (1997).
30. Brünger, A.T. *et al.* Crystallography & NMR System (CNS): a new software system for macromolecular structure determination. *Acta Crystallogr. D* **54**, 905–921 (1988).
31. Tong, L. Combined molecular replacement. *Acta Crystallogr. A* **52**, 782–784 (1996).
32. Navaza, J. & Saludjian, P. AMoRe: an automated molecular replacement program package. *Methods Enzymol.* **276**, 581–594 (1997).